

Performance Simulation of Side-Pumped Slanted Faces of High Power Yb:YAG\YAG Thin-Disk Laser

H. Aminpour* and A. Hojabri

Department of Physics, Karaj Branch, Islamic Azad University, Karaj, Iran

*Corresponding Author: ph_matnava@yahoo.de

ABSTRACT— We present a novel slanted faces of thin-disk composite Yb:YAG \ YAG laser which is side-pumped by four non-symmetric hollow- ducts. The pump light distribution in the disk is modeled by using Monte-Carlo ray tracing method. The temperature distribution inside the crystal is calculated by taking into account either the concentration of Yb^{+3} ion or the different transmission of laser output coupler. By using Finite Element Analysis (FEA) method, we calculated the absorption efficiency through the disk. The resonator is simulated by self consistently method. The resulting of optical efficiency and the output power of our laser have been modeled.

KEYWORDS: Edged-pumped thin disk laser, Monte-Carlo ray tracing, optical to optical efficiency.

I. INTRODUCTION

According to several advantages of Yb:YAG crystal, It has been a promising candidate for high – power laser diode – pumped solid state laser [1, 2]. High average power have been obtained with high efficiency by using different laser cavity configurations, such as end-pumped microchip lasers, edge-pumped and side- pumped laser systems [3-6]. The main disadvantage of ytterbium-doped material is their quasi three-level nature caused by the thermal population of terminated lasing level [7]. This effect becomes worse at high temperature induced from the heat generated by the absorbed pump power inside the Yb:YAG crystal. The thermal conductivity of Yb:YAG crystal decreases and the thermal loading parameter increases with increasing ytterbium concentration . In addition, there is

strong emission quenching, which is attributed to uncontrolled impurities during crystal growth. These concentration dependent thermal properties of Yb:YAG have great unwanted effects on the laser performance of side – pumped Yb:YAG disk laser. The thermal conductivity, thermal expansion coefficient and thermal loading of Yb:YAG crystals related to the temperature. The temperature increment which is induced by the pump power deposited on the gain medium is critical factor to be considered in the laser performance of side-pumped Yb:YAG high power disk laser. Some numerical and analytical calculations of ytterbium concentration in side – pumped slab geometry have been affected by Eggleston *et al.* [8], and Kane *et al.* [9]. Also, Rutherford *et al.* gave an analytic description of edged-pumped quasi – three level slab laser based on the assumption of the laser material’s temperature-independent absorption coefficient [10]. The work by Rutherford *et al.* [10] presented a compromise between pump absorption efficiency and uniformity as a function of the product of the absorption coefficient and the slab width. In addition, Chen *et al.* explored a method of using gradient doping concentration to optimize the pumping efficiency and the pumping uniformity in edged- and end pumped slab lasers , separately [11, 12]. Dong *et al.* reported on the effect of Yb^{3+} -ion concentration on the performance of end – pumped Yb:YAG microchip lasers at ambient temperature [13]. Dong *et al.* have demonstrated the lower the Yb concentration, the better on the lasing of YAG crystal with different dopant at high pump power level.

In Ref. [13], a 1-mm-thick Yb:YAG crystal with 10 At. % Yb³⁺ ion of microchip laser at ambient temperature is described.

Different output powers and crystal structures such as microchip composite [14] and ceramic microchip [15] lasers have been reported for efficient edged-pumped thin disk laser. In Ref. [15], Taira *et al.* presented a square composite microchip with an un-doped cap layer surrounding the core material for better heat conduction. Recently, the new geometry of side - pumped thin disk laser is presented by our group [16]. The structure of the gain medium which are side-pumped slanted sides with an un-doped cap on the active medium are applied to achieve high output power and obtain better efficiency in our delivery system. In this work, temperature-dependent and temperature-independent absorption coefficients are presented. Then, the related consequence of output power due to different transmission of output coupler and different concentration of Yb³⁺-ions calculated.

II. PROCESS OF THE WORK

In this work, the side-pumped slanted faces disk laser was carried out with a 0.2- mm-thick Yb:YAG crystal doped with 5, 10, 15, and 20 At. % Yb³⁺ ions as a gain medium. Also, a 1.3-mm-thick YAG crystal bonded on the gain medium and has a role of un-doped cap to reduce the ASE effect in the gain medium. In the manner of edged-pumped of this specific shape of disk laser, we used four non-symmetric hollow- ducts [16]. The schematic diagram of the set up illustrated in Fig. 1(a). The bottom surface of the disk is highly-reflection-coated at both 941 nm and 1030 nm to act as a rear mirror of the cavity. A concave-plane mirror was used as output coupler with different transmissions (T_{oc}) of 3, and 10% at 1030 nm.

The overall cavity length was 400 mm in linear setup as shown in Fig. 1(b). Four high power stacked LD in 941 nm with output divergence about 0.25° and 10° of fast axis and slow axis respectively were used as the pump sources. About 96% of the total pumping power is incident on the Yb:YAG

crystal after passing through the non-symmetric hollow-ducts.

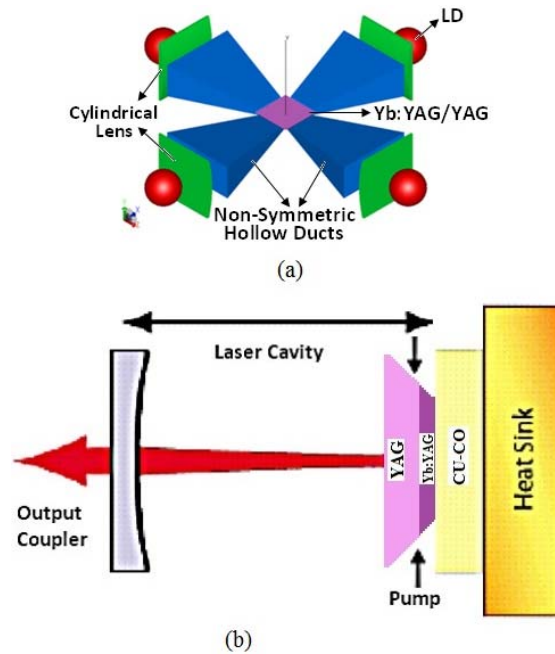


Fig. 1. (a) Schematic diagram of Yb:YAG/YAG edged-pumped disk laser with four non-symmetric hollow ducts and (b) The cavity setup used in the simulation.

The numerical simulation which is used for our CW-operation of the thin disk laser consists of four distinct steps [17]. The first step is to calculate the distribution of absorbed pump power within the crystal. This is done by using Monte-Carlo-ray tracing method. We taking into account the changes of absorption efficiency with crystal temperature and population inversion of the system. The second step is to calculate the temperature within the crystal that results from energy conversion loss between pump and laser energy. In the third and fourth steps the population inversion and the output power are calculated respectively. Assuming by an ideal plane-parallel and infinitesimal short resonator, the last two steps have been calculated. We should to notice that, steps one through three are iterated until a steady state is reached.

III. NUMERICAL SIMULATION OF THE CW-OPERATION OF THE THIN DISK LASER

The distribution of absorbed pump energy within the crystal is calculated by means of Monte-Carlo-ray tracing. This means that the path of randomly generated pump photons is followed through the optical system regarding the absorption as a statistical process. We used 10000 random photons for each pump sources.

It means that every photon starts with a random position on the entrance slanted facets of the non-symmetrical hollow ducts. A random moving direction which is determined following the calculated angle distribution of a hollow duct which is determined according to an assumed Gaussian profile with the spectral width of the diodes. The path of the photon is then followed through the crystal until it is absorbed completely. Remaining of the photons regards to the geometry of the gain medium are trapped on the internal front slanted surface of the gain medium and again reabsorbed in returning direction through the disk. Then, the absorbed photons are counted in elements of a mesh into which the crystal is divided. In our modeling a mesh consists of 13 layers perpendicular to the crystal axis (z-axis), 110 squares in length direction (X-axis) and the same meshing for width direction (Y-direction) of the gain medium. We used typically triangular meshing structure in slanted facets of the gain medium for doing realistic simulation of the disk. In order to determine whether a passing photon is absorbed, its way through the crystal is divided into two or more steps. For each step the transmission in axial direction is calculated at Cartesian position of the photon. If the photon is absorbed, which is determined by generation

of a random number, the exact position of absorption is found by further comparison of the random number with transmission after some of the mesh elements in that step [16], Fig. 2

In Sub-section (A), we used the absorption coefficient in order to obtain the pump light distribution inside the crystal and in Sub-section (B), we have done the simulation with the temperature dependent absorption coefficient.

A. Pumping distribution with constant absorption coefficient

Related to the specific structure of the gain medium, we have done geometrical optics calculations and applied them into a ray tracing method with concentration based on the goal of the uniformity of the pump light distribution inside the gain medium. In our simulation, we supposed that, the pump light has a Gaussian spectral distribution. Also, the absorbed pump power density with the constant absorption coefficient is as a function of the position along the width of the disk.

The absorbed pump power density distribution inside the disk with constant absorption coefficient is depicted in Fig. 3. As in Fig. 3(a) shows, regarding the effect of pump absorption saturation, fewer pumps light are absorbed at the near entrance faces of the disk compare to the center of the disk. In addition, in Fig. 3(b), it is clear that the absorbed pump power density profile in X-direction and Y-direction are similar to each other and have a Gaussian profile and have a peak around the center of the disk and its value in both X- and Y-direction are 287 W/mm^3 . Furthermore, we

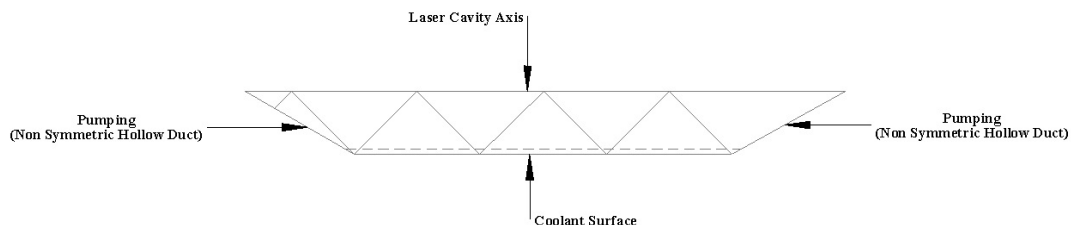


Fig. 2. Typical propagation of a photon inside the doped region (Yb:YAG) and un-doped region (YAG) used in the numerical simulation.

illustrated the 3D irradiance profile of the pump light distribution inside the disk in Fig. 3(a).

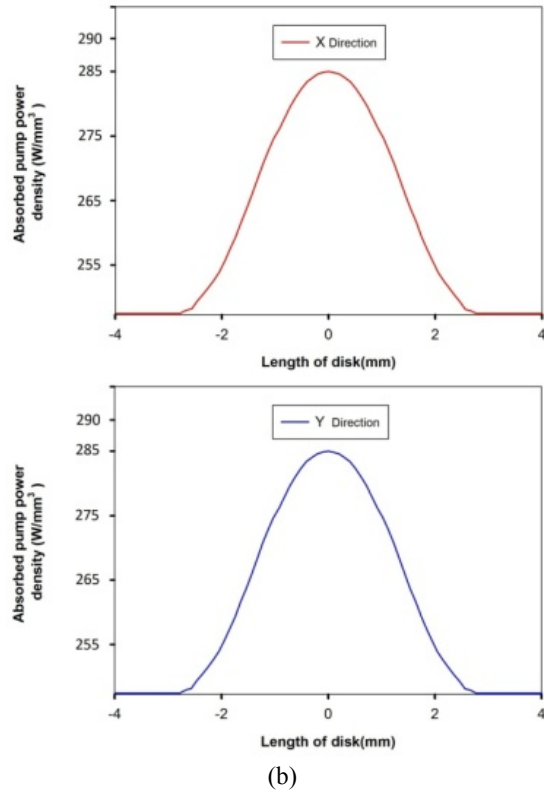
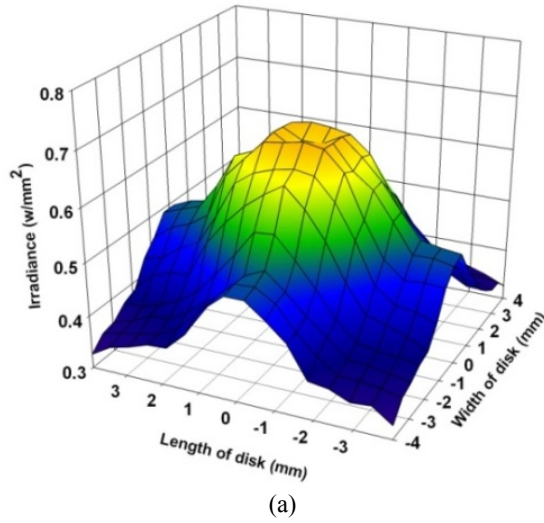


Fig. 3. Initial pump light distributions profile (a), Absorbed pump power distribution in two sides of the disk (b).

Regarding the propagation trace of the photons through the disk and also the overlapping of the rays which are reached from four hollow

ducts, one could see this effect as a deep in the irradiance profile.

B. Pumping distribution with the crystal temperature dependent absorption coefficient

Since in section A, we restricted to the case of constant absorption coefficient and do not apply to our model with the temperature-dependent absorption coefficient, we have done it in this section. The calculation of crystal temperature as a function of the absorbed energy distribution usually is symmetric around the crystal axis. So, the calculation of temperature is done for the axial- symmetry. In our simulation, the generated heat due to the quantum defect of 8.56% is taken from the calculated average absorption distribution. It is applied to the elements of a two-dimensional mesh. The resulting heat flow between every pair of neighboring elements is determined and the temperature is adjusted until the heat flow is reduced underneath a certain error limit. The heat conductivity λ is taken to be temperature dependent [18]:

$$\lambda(T) = \lambda_0 \frac{T_0 - T_{\text{off}}}{T - T_{\text{off}}} \quad (1)$$

With the heat conductivity $\lambda_0 = 13.0 \text{ W/mK}$ at $T_0 = 300\text{K}$ and $T_{\text{off}} = 42\text{K}$. The influence of the heat sink geometry is described by the value of its heat resistance. This value depends on the pump beam radius and is determined by using the finite-element-model (FEM) method on a model of the crystal and the heat sink. The final calculation of temperature distribution through the disk is illustrated in Fig. 4. Because of the axial symmetric of temperature distribution in four sides of the slanted edged pumped disk laser, we depicted a quarter of the gain medium via the whole thickness of the disk.

The absorption coefficient α can be expressed as:

$$\alpha = \alpha_0 \frac{1}{1 + (I_0/I_{\text{sat}})} \quad (2)$$

where α_0 is the small – signal absorption coefficient, I_0 and I_{sat} are the pump intensity and the Yb:YAG laser saturation intensity (at 941 nm), respectively ($I_{sat} = hv/\sigma_e\tau$), where hv is the photon energy, σ_e is the stimulated emission cross section, and τ is the excited manifold storage lifetime).

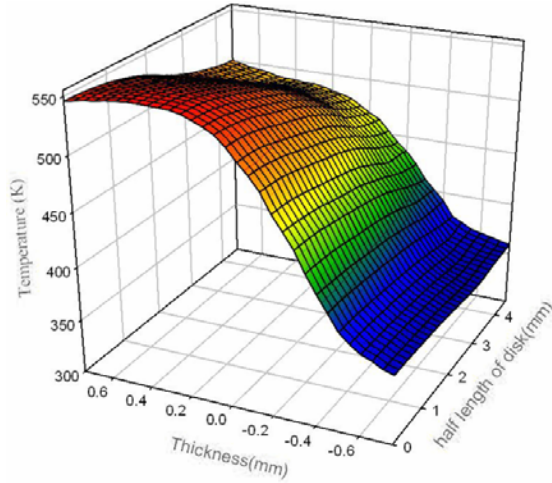


Fig. 4. Temperature distribution in the half length of the disk in a quarter section regarding the axial symmetric of the gain medium

The absorbed pump power distribution is calculated by Finite Element Analysis (FEA). The wavelength of pump light set at 941nm with Gaussian spectral distribution. The calculated results are shown in Fig. 5. As shown in Fig. 5, introduction of the temperature-dependent absorption coefficient causes the non-uniform distribution of the pump power density along the width of the gain medium. It makes the calculation of heat deposit distribution from pump power more accurate. On the other hand, we consider the dopant concentration n_d as the variable in 10, 15, 20% of Yb^{+3} ion in our calculation. So, the absorbed pump power density profile on the X-Y planes is relatively uniform.

In the following section, we used the results of previous section, in order to calculate the laser output power due to two concepts: First with different transmission of output coupler and second with different concentration of Yb^{+3} ion.

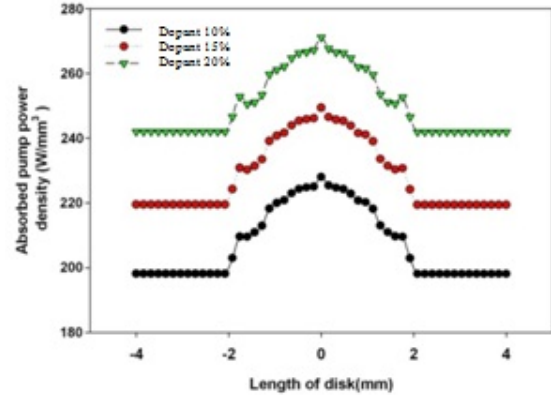


Fig. 5. Comparing of pump light absorbed distribution of Yb^{+3} ion concentrations for 10, 15, and 20% respectively through the disk.

IV. LASER OUTPUT POWER CALCULATION AND OPTICAL EFFICIENCY OF THE DISK

A. Different transmission of output coupler

Based on the work reported by Beach [20] and Rutherford *et al.* [10], we calculate the output power of an edged-pumped quasi-three level thin disk laser. Besides the effects of lower manifold depletion, output coupling, temperature – dependent thermal conductivity and pump absorption saturation our particular structure of the gain medium consider to the thermal effects of the laser output power [21]. The considered case is of multiple transverse mode oscillation, where the laser mode nearly fills the disk.

The data stands for our configuration which are used as the basis of our calculations are given in Table 1. [19]; [20].

Therefore, the laser output power can be written as a function of the pump power as given by [20].

$$P_{out} = \eta_{Slope} (\eta_{abs} P_p - P_0) \quad (4)$$

where, P_{out} is the laser output power, P_p is the pump power, η_{Slope} is the slope factor, η_{abs} is the pump efficiency and P_0 is the threshold factor. The terms of η_{Slope} , η_{abs} and P_0 are given in [22]. The expression of P_{out} as referred to (6), shows the temperature dependence of three parameters: Boltzmann

population fractions (f_a, f_b, f'_a, f'_b), stimulated emission cross section (σ_e) and absorption coefficient (σ_{abs}).

TABLE 1 DATA USED FOR OUR MODELING

Parameter	Value	
Crystal thickness (doped-region)	200	(μm)
Cap thickness (undoped-region)	1.3	(mm)
Dopant concentration (C_{Yb})	5, 10, 15, 20	(%)
Number of non-symmetric hollow-duct	4	(pics)
Pump Wavelength (λ_p)	941	(nm)
Number of Pump beam pass	16	
Temperature of cooling fluid (T_c)	286	(K)
Fluorescence lifetime [20]	950	(μs)
Heat conductivity ($\lambda @ 300\text{K}$)	13.0	($\text{Wm}^{-1}\text{K}^{-1}$)
Reflectivity of output coupler (R)	3, 5, 10, 15	(%)
Resonator internal losses (L)	~ 0.2	(%)
Linear expansion coefficient [21]	6.9×10^{-6}	
Crystal thickness (doped-region)	200	(μm)
Cap thickness (undoped-region)	1.3	(mm)
Dopant concentration (C_{Yb})	5, 10, 15, 20	(%)
Number of non-symmetric hollow-duct	4	(pics)
Pump Wavelength (λ_p)	941	(nm)

The Boltzmann occupation factors of pump and laser levels depending on the temperature are expressed as follows [22]:

$$f_a = \frac{\exp\left(-\frac{E_a^L}{KT}\right)}{\sum \exp\left(-\frac{E_i}{KT}\right)}, \quad f_b = \frac{\exp\left(-\frac{E_b^L}{KT}\right)}{\sum \exp\left(-\frac{E_j}{KT}\right)} \quad (5)$$

where the sums are done over all the Stark levels of the ground manifold, and

$$f'_a = \frac{\exp\left(-\frac{E_a^P}{KT}\right)}{\sum \exp\left(-\frac{E_i}{KT}\right)}, \quad f'_b = \frac{\exp\left(-\frac{E_b^P}{KT}\right)}{\sum \exp\left(-\frac{E_j}{KT}\right)} \quad (6)$$

where, the sums are shown over all Stark levels of the excited manifold. E_a^P and E_b^P are energies for the lower and the upper pump Stark levels, E_a^L and E_b^L are energies for the lower and the upper laser Stark levels, respectively. K is the Boltzmann constant, E_i is the energy for each Stark level of the ground manifold and E_j is the energy for each Stark level of the excited manifold.

The temperature dependence of σ_e for Yb:YAG has been given by Chen *et al.* [12].

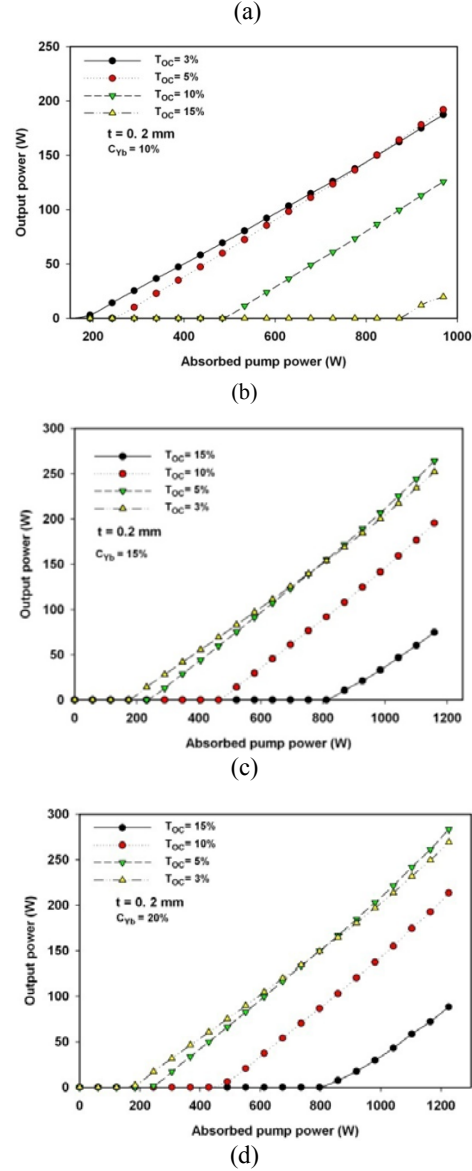


Fig. 6. Output power of Yb:YAG/YAG disk laser as a function of the absorbed pump power for Yb:YAG crystals doped with different output coupler transmissions. (a) $C_{Yb}=5$ At. %, (b) $C_{Yb}=10$ At. %, (c) $C_{Yb}=15$ At. %, $C_{Yb}=20$ At. %.

The output power of Yb:YAG disk laser as a function of the absorbed pump power for $T_{oc} = 3, 5, 10, 15\%$ is shown in Fig. 6. For the case of $C_{Yb} = 5\%$, the transmission of output coupler (T_{oc}) are 2, 3, 4 and 5% due to the absorbed pump power thresholds of 0.2 – mm – thick disk laser. The absorbed pump power threshold of 0.2-mm-thick Yb:YAG laser is

183 W for 20 atomic % of ytterbium concentration.

As shown in Fig. 6, the output power increase linearly with the absorbed pump power when the pump power is well above the pump power threshold for Yb:YAG crystal doped with 10, 15, and 20 At. % Yb³⁺. This effect is respect to the nature of quasi-three level operating scheme. Also, high efficiency can be achieved by using high pump power intensity. There is a drop of the slop efficiency for 10 At. % Yb:YAG thin disk laser, which is caused by the low transmission of output coupler. For 15, 20 At. % Yb:YAG, the output power increase linearly with absorbed pump power when the absorbed pump power is lower than 183 W and 231 W for T_{oc}= 3%, respectively. In Fig. 6(a), the highest slop efficiency (with respect to the absorbed pump power) of 24 % was achieved by using T_{oc}= 2% for C_{Yb} = 5 At. %. where, the optical- to- optical slope efficiency of 40% is obtained. According to the high pump power threshold of Yb:YAG disk lasers, we obtained the output power by increasing one-step of output coupler transmissions from 2% to 5%. In Fig. 6(b), we calculate the output power for c_{Yb}=10 At. %, due to different transmission of output coupler.

TABLE 2 Performance of Yb:YAG side-pumped slanted – faces disk laser with different Yb³⁺ dopant. λ_L , laser emitting wavelength ; P_{th}, Power threshold ; P_{abs}, Absorbed pump power ; P_{out}, Maximum output power ; $\eta_{O-O(a)}$, Maximum optical – to – optical efficiency corresponding to absorbed pump power.

Yb:YAG	T _{oc} (%)	λ_L (nm)	P _{th} (W)	P _{abs} (W)	P _{Out} (W)	η_{Slope} (%)	$\eta_{O-O(a)}$ (%)
5 At.%, 0.2 mm- thick	2	1030	504	673.3	158	24	40
	3	1030	538	673.3	138	20	40
	4	1030	605	673.3	117	17	40
	5	1030	673	673.	75	11	40
10 At.%, 0.2 mm- thick	3	1030	192	969.2	188	19	53
	5	1030	289	969.2	192	21	53
	10	1030	533	969.2	126	13	53
15 At.%, 0.2 mm- thick	15	1030	920	969.2	20	0.02	53
	3	1030	231	1159	285	24	63
	5	1030	288	1159	288	25	63
	10	1030	520	1159	196	16	63
20 At.%, 0.2 mm- thick	15	1030	869	1159	75	0.06	63
	3	1030	183	1226	295	24	67
	5	1030	245	1226	296	24	67
10	1030	490	1226	214	17	67	
	15	1030	858	1225	89	0.07	67

Also, we obtained the highest slop efficiency of 21% by using T_{oc}= 5%. For this case the

optical – to – optical slope efficiency is 53%. By increase of Yb³⁺ concentrations to 15%, we obtained the output power of 288 W with slope efficiency (respect to the absorbed pump power) of 25% and the optical – to – optical slope efficiency of 63% Fig.6(c). In Fig. 6(d), we used 20% of Yb³⁺ concentrations due to different output coupler transmission for 3, 5, 10, 15 % respectively. The highest output power were obtained 296 W with the optical – to – optical slope efficiency of 67% and the slope efficiency with respect to the absorbed pump power of 24%.The output power and slope efficiency (with respect to the absorbed pump power) with different At.% of Yb³⁺ ions concentration are also listed in Table 2.

B. Different concentration of Yb³⁺ ion

The output power calculation respect to the absorbed pump power in different of Yb³⁺ ion concentration of c_{Yb} = 10, 15 and 20 At. % have been done. We use different transmission of output coupler of 3, 10 and 15 At. %, respectively. The results of the output power calculation are illustrated in Fig. 7(a, b, c). As shown in Fig. 7(a), the highest output power is obtained for c_{Yb} = 20 At. % for T_{oc} = 15% with the slop efficiency of 10%. In Fig. 7(b), the output power calculation due to the transmission of the output coupler (10%) in different concentration of Yb³⁺ ion is depicted. we obtained the highest output power for the c_{Yb} = 20 At. %. However, by use of c_{Yb} = 15 At. % the output power calculation is near to the use of c_{Yb} = 20 At. %. The slope efficiency (respect to the absorbed pump power) of 31% and optical – to – optical slope efficiency of 75% were obtained. By decreasing the output coupler transmission into 3%, we calculated the output power. The results is depicted in Fig. 7(c). As shown in Fig. 7 (c), for Toc = 3% the output power of c_{Yb} = 15 and 20 At. % were calculated whereby we show that there are nearly similar to each other. The optical – to – optical slope efficiency of 54% and the slope efficiency (respect to the absorbed pump power) of 30% have been obtained. By comparing the results in Fig. 7(a, b, c), the output power threshold has been decreased for c_{Yb} = 20 At. % from 640 W to 197W corresponding to the decrease of output

coupler transmission from $T_{oc} = 15\%$ to $T_{oc} = 3\%$.

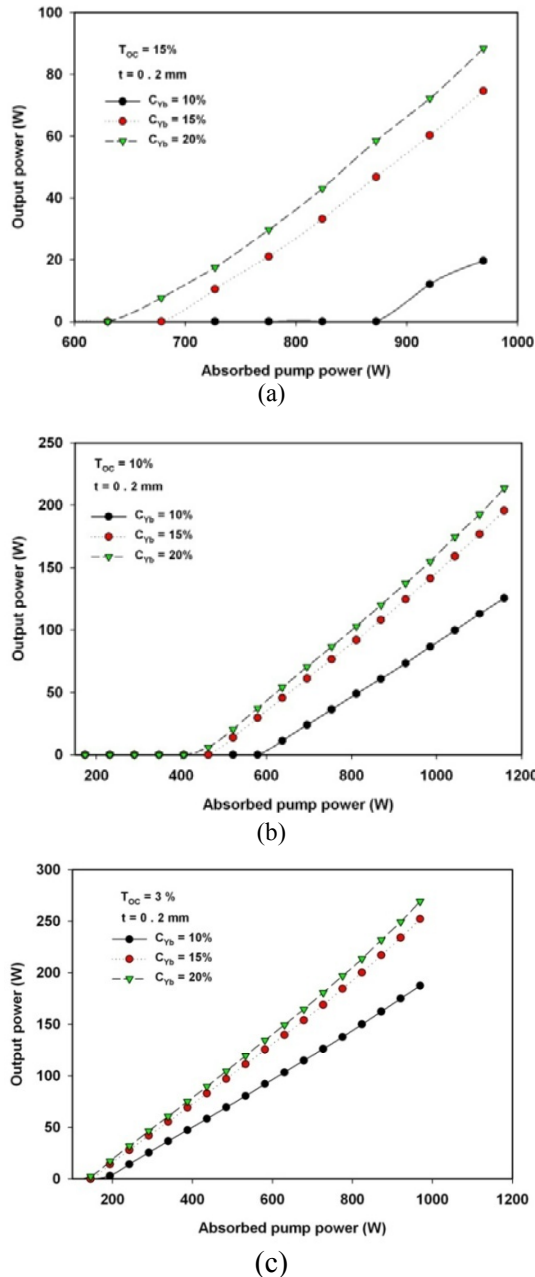


Fig. 7. The output power of Yb:YAG/YAG disk laser as a function of the absorbed pump power for Yb:YAG crystals doped with different Yb³⁺ concentrations in thickness of 0.2 mm. (A) $T_{oc} = 3\%$, (B) $T_{oc} = 10\%$, (C) $T_{oc} = 15\%$.

V. CONCLUSION

In this paper, we present a side-pumped slanted faces of high power Yb:YAG/YAG thin disk laser which is pumped by the manner of non-symmetric hollow ducts. Distribution

of pump light and absorbed pump power in the active medium are calculated by the use of Monte-Carlo ray tracing and Finite Element Analysis (FEA) methods, respectively. By using the results of FEA, the output power of the gain medium is calculated in two following steps: First, respect to the different value of the output coupler transmission and second with different concentration of Yb³⁺ ion. For those two steps we solved the rate equation for three-level lasing medium. Finally, by comparing the results one can understand from the table the slope efficiency of the side pumped slanted faces Yb:YAG/YAG high power thin disk laser.

ACKNOWLEDGMENTS

The authors of this paper would like to express their fully thanks to the collaborations of I. Mashaieky Asl and M. Esmaili in INLC during the preparation of this work.

REFERENCES

- [1] A. Giesen, H. Hügel, A. Voss, K. Wittig, U. Brauch, and H. Opower, "Scalable Concept for Diode-Pumped High-Power Solid-State Lasers," *Appl. Phys. B* Vol. 58, pp. 365-372, 1994.
- [2] T.S. Rutherford, W.M. Tulloch, E.K. Guastafson, and R.L. Byer, "Edged-Pumped Quasi-Three-Level Slab Lasers: Design and Power Scaling," *IEEE J. Quantum Electron.* Vol. QE-36, pp. 205-219 2000.
- [3] E.C. Honea, R.J. Beach, S.C. Mitchell, J.A. Sidmore, M.A. Emanuel, S.B. Sutton, S.A. Pyne, P.V. Avizonis, R.S. Monroe, and D. Harris, "High-power dual-rod Yb:YAG laser," *Opt. Lett.* Vol. 25, pp. 805-807, 2000.
- [4] C. Stewen, K. Contag, M. Larinov, A. Giesen, and H. Hugel, "Role of undoped cap in the scaling of thin-disk lasers," *IEEE J. Sel. Top. Quantum Electron.* Vol. 6, pp. 650-657, 2000.
- [5] M. Tsunekane and T. Taira, "300 W continuous-wave operation of a diode edge-pumped, hybrid composite Yb:YAG microchip laser," *Opt. Lett.* Vol. 31, pp. 2003-2005, 2006.
- [6] H. Bruesselbach and D.S. Sumida, "A 2.65-kW Yb:YAG single-rod laser," *IEEE J. Sel.*

- Top. Quantum Electron. Vol. 11, pp. 600-603, 2005.
- [7] A. Bogomolova, D.N. Vylegzhanin, and A.A. Kaminskii, "Spectral and lasing investigations of garnets with Yb^{3+} ion," Sov. Phys. JETP Vol. 42, pp. 440-446, 1967.
- [8] J.M. Eggleston, T. J. Kane, K. Kuhn, J. Unternahrer, and R. L. Byer, "The slab geometry laser-Part I: theory," IEEE U. Quantum Electron. QE-20, 289-300, 1984.
- [9] T.J. Kane, J.M. Eggleston, and R.L. Byer, "The slab geometry laser-Part II: thermal effects in a finite slab," IEEE J. Quantum Electron. Vol. QE-21, pp. 1195-1210, 1985.
- [10] T.S. Rutherford, W.M. Tulloch, S. Sinha, and R.L. Byer, "Yb:YAG and Nd:YAG edge-pumped slab lasers," Opt. Lett. Vol. 26, pp. 986-988, 2001.
- [11] B. Chen, Y. Chen, and M. Bass, "Edged- and end-pumped slab lasers with both efficient and uniform pumping," IEEE J. Quantum Electron. Vol. 42, pp. 483-489, 2006.
- [12] B. Chen, J. Dong, M. Patel, Y. Chen, A. Kar, and M. Bass, "Modeling of high power solid-state slab lasers," Proc. SPIE 4968, pp. 1-10, 2003.
- [13] J. Dong, A. Shirakawa, K.I. Ueda, and A.A. Kaminskii, "Effect of ytterbium concentration on CW Yb:YAG microchip laser performance at ambient temperature- Part I: Experiments," Appl. Phys. B: Lasers and Opt. Vol. 89, pp. 359-365, 2007.
- [14] D. Kracht, D. Freiburg, R. Wilhelm, M. Frede, and C. Fallnich, "Core doped Ceramic Nd:YAG laser", Opt. Express, Vol. 14, pp. 2690-2692, 2006.
- [15] M. Tsunekane and T. Taira, "High - power operation of diode edge-pumped, composite all -ceramic Yb: Y3Al5 O12 microchip laser," Appl. Phys. Lett. Vol. 90, pp. 121101-121103, 2007.
- [16] H. Aminpour, I. Mashaieky Asl, J. Sabbaghzadeh, and S. Kazemi, "Simulation and design of applied hollow-duct used for side-pumped cutting-edged of high power disk laser," Opt. Commun. Vol. 283, pp. 4727-4732, 2010.
- [17] K. Contag, U. Brauch, S. Erhard, A. Giesen, I. Johannsen, M. Karszewski, C. Stewen, and A. Voss, "Simulations of the Lasing Properties of a Thin Disk Laser combining High Output Powers with Good Beam Quality", Proc. SPIE 2986, pp. 23-34, 2003.
- [18] G.A. Slack and D.W. Oliver, "Thermal Conductivity of Garnets and Phonon Scattering by Rare-Earth Ions," Phys. Rev. B Vol. 4, pp. 592-609, 1971.
- [19] D.S. Sumida and T.Y. Fan, "Emission Spectra and Fluorescence Lifetime Measurements of Yb:YAG as a Function of Temperature," OSA Proc. on Advanced Solid-State Lasers Vol. 20, pp. 100-102, 1994.
- [20] R.J. Beach, "CW theory of quasi-three level end- pumped laser oscillators," Opt. Commun. Vol. 123, pp. 385-393, 1996.
- [21] Q. Liu, X. Fu, M. Gong, and L. Huang, "Effects of the temperature dependence of absorption coefficients in edge-pumped Yb:YAG slab lasers," J. Opt. Soc. Am. B, Vol. 24, pp. 2081-2089, 2007.
- [22] W. Koechner, *Solid- State Laser Engineering*, 5th ed. Springer-Verlag, 1999.



Hamed Aminpour, born on 1982 in Karaj, Iran. He received his B.Sc. degree in Physics from Instructor Training Center University (ITC), Iran, in 2008 and the M.Sc. degree in Condensed Matter of Physics from Azad University, Iran, in 2011.

He has worked on diode-laser-pumped solid state lasers toward his M.Sc. thesis in Iranian National Center for Laser Science and Technology (INLC). He is currently joining to his supervisor's laboratory group as a part time researcher at Azad University, Karaj, Iran. His present research interests are focused on numerical calculation of Optical Path Difference (OPD) and calculation of Amplified Spontaneous Emission (ASE) effects in solid state lasers. Mr. Hamed Aminpour is a member of Optical Society of

America (OSA), SPIE, European Optical Society (EOP) and Optics and Photonics Society of Iran (OPSI).



Alireza Hojabri was born in Tehran, Iran on January 1968. He received his B.Sc. degree in Solid State Physics from the Islamic Azad University of Karaj, Iran, in 1990 and M.Sc. degree in Solid State Physics from Islamic

Azad University of Tehran, Iran in 1992. He was doing his researches toward Ph.D. degree in Science and Research Campus of Islamic Azad University, Tehran Iran. He presented his Ph.D. thesis “On the Investigation of Major Disruption and Mode locking in Iran-Tokamak 1 (IR-T1)” and received his Ph.D. degree in September 2000. Since May 1993, he has been working in Physics Department of Islamic Azad University in Karaj, Iran as an academic member, from November 2002 to 2005, he was deputy of the Faculty of Science, and since 2005, he is dean of the Faculty of Science there. He has published over 30 technical papers in scientific journals. His research is concentrated on Plasma Physics, Thin Films and Solid State Physics.